Article

J. Biol. Regul. Homeost. Agents. 2024; 38(1): 111–122
https://doi.org/10.23812/j.biol.regul.homeost.agents.20243801.8

The Different Effects of Pharmacological or Low-Doses of IFN-γ on Endothelial Cells are Mediated by Distinct Intracellular Signalling Pathways

Alessandra Cazzaniga[1], Vincenzo Miranda[2], Sara Castiglioni[1,*], Jeanette A. Maier[1]

[1]Department of Biomedical and Clinical Sciences, Università di Milano, 20157 Milan, Italy
[2]Clinical Research Unit, GUNA S.p.a., 20132 Milan, Italy
*Correspondence: sara.castiglioni@unimi.it (Sara Castiglioni)
Published: 1 January 2024

Background: Interferon (IFN)-γ is a proinflammatory cytokine with a crucial role in intercellular communication during innate and acquired immune responses. IFN-γ interacts with various cell types, including endothelial cells. Here, we investigated the effects of pharmacological or low doses of IFN-γ in cultured endothelial cells.
Methods: Human endothelial cells were cultured in the presence of pharmacological or low-dose concentrations of IFN-γ. Signal transducer and activator of transcription (STAT) and Extracellular signal-regulated kinase (ERK) phosphorylation were investigated by enzyme linked immunosorbent assay (ELISA). Western blot for ERK was also performed. Transient ERK silencing was obtained by short interfering RNA (siRNA). Cell proliferation and migration were analysed by cell counting and wound assay, respectively.
Results: At pharmacological concentrations, IFN-γ activates the Janus kinases (JAK)/STAT pathway, leading to the overexpression of the cyclin-dependent kinase inhibitor 1A/p21 (*CDKN1A/p21*), which inhibits cell growth. In contrast, low-dose activated IFN-γ does not trigger the canonical JAK/STAT pathway and induces the phosphorylation of ERK. ERK activation is responsible for endothelial cell migration induced by low-dose activated IFN-γ.
Conclusions: We demonstrate that pharmacological and low-dose activated IFN-γ exert distinct effects on endothelial cells by triggering different signal transduction pathways. These findings shed light on the intricate signalling pathways employed by IFN-γ, and suggest that low-doses of IFN-γ might play a homeostatic role in endothelial cell during innate and acquired immune responses.

Keywords: interferon γ; endothelial cells; ERK; STAT; migration

Introduction

The endothelium is a dynamic, disseminated organ which performs essential functions. In addition to acting as a physical barrier between the blood and the tissues, vascular endothelial cells (EC) modulate metabolic homeostasis, control coagulation and vascular tone. Moreover, EC play a central role in the regulation of local immune and inflammatory reactions. Vascular EC synthesize and release components of the complement cascade [1]. Moreover, EC are a source and a target of chemokines and cytokines, and, when activated, express both Toll-like receptors (TLRs) and nucleotide-binding oligomerization domain (NOD)-like receptors (NLRs) as well as adhesion molecules for leukocytes [2], thus regulating immune cell recruitment to specific inflammatory sites. For this reason, EC were proposed as conditional innate immune cells [2]. Because of their location, EC are one of the first targets of cytokines circulating in the blood stream. They respond to interferon (IFN)-γ, a pro-inflammatory cytokine crucial in intercellular communication during innate and acquired immune responses [3]. Indeed, like most cells in the body, EC express the IFN-γ receptor (IFN-γR) [3]. Similarly to several other cytokine receptors, IFN-γR primarily signals through the engagement of the Janus kinase/Signal transducer and activator of transcription (JAK/STAT) pathway. In brief, STAT-1 is phosphorylated by the JAK-2, forms homodimers, translocates to the nucleus and binds to the γ-activated sequence elements (GAS elements) within the promoters of IFN-γ-responsive genes [3,4]. STAT-1 also interacts with other transcription factors, such as STAT-2 and interferon regulatory factor (IRF)-9, to form heterodimers and modulate transcription [5,6]. Moreover, since IFN-γ stimulates gene expression in STAT-1-/- macrophages [7], noncanonical IFN-γ signalling pathways have been described. The activation of these alternative pathways, which include small G proteins and Mitogen-activated protein kinases (MAPK), requires long duration treatments (hours rather than minutes) with IFN-γ [8].

Journal of
BIOLOGICAL REGULATORS
and Homeostatic Agents

In EC, IFN-γ modulates the expression of hundreds of genes [9], among which TNF-related apoptosis-inducing ligand (TRAIL), guanylate binding protein (GBP)1, and the chemokines CXCL10 and 11 [9]. This transcriptional program induced by IFN-γ might account for the widely reported inhibition of endothelial proliferation *in vitro* [10–12] as well as for its angiostatic effects *in vivo* [13]. It has been shown that IFN-γ induces non apoptotic blood vessel regression in development and wound healing, and has a role in remodelling of uterine vessels during pregnancy [14–16] as well as in experimental models of cancer [13]. The activation of the STAT-1 signalling is required for growth inhibition, as short interfering RNA (siRNA) targeting *STAT-1* abrogated IFN-γ-induced inhibition of EC growth [17]. STAT-1 activation also mediates the increase of endothelial permeability by redistributing junctional proteins and stimulates the transmigration of lymphocytes through the endothelial barrier [18]. Of interest, 24 hour treatment with IFN-γ is necessary to activate p38 MAPK in EC and rearrange the cytoskeleton [19].

In these experimental settings the concentrations of IFN-γ utilized are much higher than the ones detected *in vivo* [20–22]. Evidence is accumulating that ligand concentrations from 10^{-18} M to 10^{-24} M induce biological responses in various biological systems [23]. However, the quantitative insight into the number of cytokine molecules needed to activate a target cell has been overlooked. A recent report demonstrates that interleukin (IL)-6 signalling requires only few IL-6 molecules [24]. This is likely to be true for most cytokines, including IFN-γ, in physiological conditions. It should also be recalled that, in spite of its enormous therapeutic potential in immune diseases and in cancer, the use of IFN-γ is limited by its dose-dependent side effects [25]. We have previously shown that very low-doses of IFN-γ exert an immunomodulatory action in Jurkat cells [26]. Here we compare the effects of different concentrations of IFN-γ on the behaviour of human EC.

Materials and Methods

Cell Culture

Primary Human Umbilical Vein Endothelial Cells (HUVEC) were from Lonza (Catalogue no. C2519A, Lonza, Basilea, Switzerland) and cultured in EBM™ Basal Medium supplemented with EGM™ Endothelial Cell Growth Medium SingleQuots™ (Catalogue no. 3162, Lonza, Basilea, Switzerland) on 2% collagen-coated dishes. Cells used in this study are free of contamination by STR and mycoplasma testing. HUVEC were treated with two different formulations of IFN-γ (Catalogue no. C-60724, PromoCell, Heidelberg, Germany) as previously reported: an activated solution and a non-activated solution. After sequential serial dilution (1:100) in 30% hydroalcoholic solution, on the basis of previous knowledge on activated blends [27,28] the activation was attained by a shaking procedure (vertical shaking; 10 cm motion range; shaking speed corresponding to 100 oscillations in 10 seconds). IFN-γ activated (A-IFN-γ) or not (IFN-γ) was used at pharmacological (10 ng/mL) or low-dose (10 pg/mL) concentrations [28]. For proliferation experiment, 20 × 103 cells/cm^2 were seeded in 24-well plates and treated with pharmacological or low-dose concentrations of the activated and non-activated formulations of IFN-γ. After different time points, the cells were stained with Trypan blue solution (0.4%) (Catalogue no. T8154, Sigma Aldrich, St. Louis, MO, USA), and the viable cells were counted using a cell counter. Nifuroxazide (Catalogue no. 481984, Calbiochem, St. Louis, MO, USA) (3 μM for 16 h) was used to inhibit STAT-1 [29]. The concentration of 3 μM was chosen because it exerts no cytotoxicity in HUVEC (not shown). The experiments were performed three times in triplicate.

qRT-PCR

Total RNA was extracted by the PureLinkRNA MiniKit (Catalogue no. 12183018A, Thermo Fisher Scientific, Waltham, MA, USA). Single-stranded cDNA was synthesized from 1 μg RNA in a 20 μL final volume using the High-Capacity cDNA Reverse Transcription Kit (Catalogue no. 4368814, Thermo Fisher Scientific, Waltham, MA, USA), according to the manufacturer's instructions. Real-time Quantitative Reverse Transcription PCR (qRT-PCR) was performed three times in triplicate using the CFX96 Touch Real-time Quantitative Reverse Transcription PCR Detection System (Bio-Rad, Hercules, CA, USA) instrument utilizing the TaqMan Gene Expression Assay (Catalogue no. 4351370, Life Technologies, Monza, Italy). The following primers were used: Hs00355782_m1 cyclin-dependent kinase inhibitor 1A/p21 (*CDKN1A/p21*) and Hs99999905_m1 Glyceraldehyde-3-Phosphate Dehydrogenase (*GAPDH*) was used as an internal reference gene. Relative changes in gene expression were analysed by the $2^{-\Delta\Delta Ct}$ method.

Western Blot Analysis

HUVEC were lysed in lysis buffer (50 mM Tris-HCl pH 8.0, 150 mM NaCl, 1 mM EDTA, 1% Nonidet P40 Substitute). Protein concentration was determined using the Bradford reagent (Catalogue no. B6916, Sigma Aldrich, St. Louis, MO, USA). Equal amounts of proteins were separated by SDS-PAGE and transferred to nitrocellulose membranes by using Trans-Blot Turbo™ Transfer Pack (Catalogue no. 1704158, Bio-Rad, Hercules, CA, USA). Western blot analysis was performed using primary antibodies against p-Extracellular signal-regulated kinase (ERK) (dilution 1:1000, Catalogue no. sc-7383, Cell Signaling Technologies Danvers, MA, USA), ERK1/2 (dilution 1:200, Catalogue no. sc-154, Santa Cruz Biotechnology, Dallas, TX, USA) and β-actin (dilution 1:1000, Catalogue no. sc-47778, Santa Cruz Biotechnology, Dallas, TX, USA). Secondary antibodies conjugated with horseradish perox-

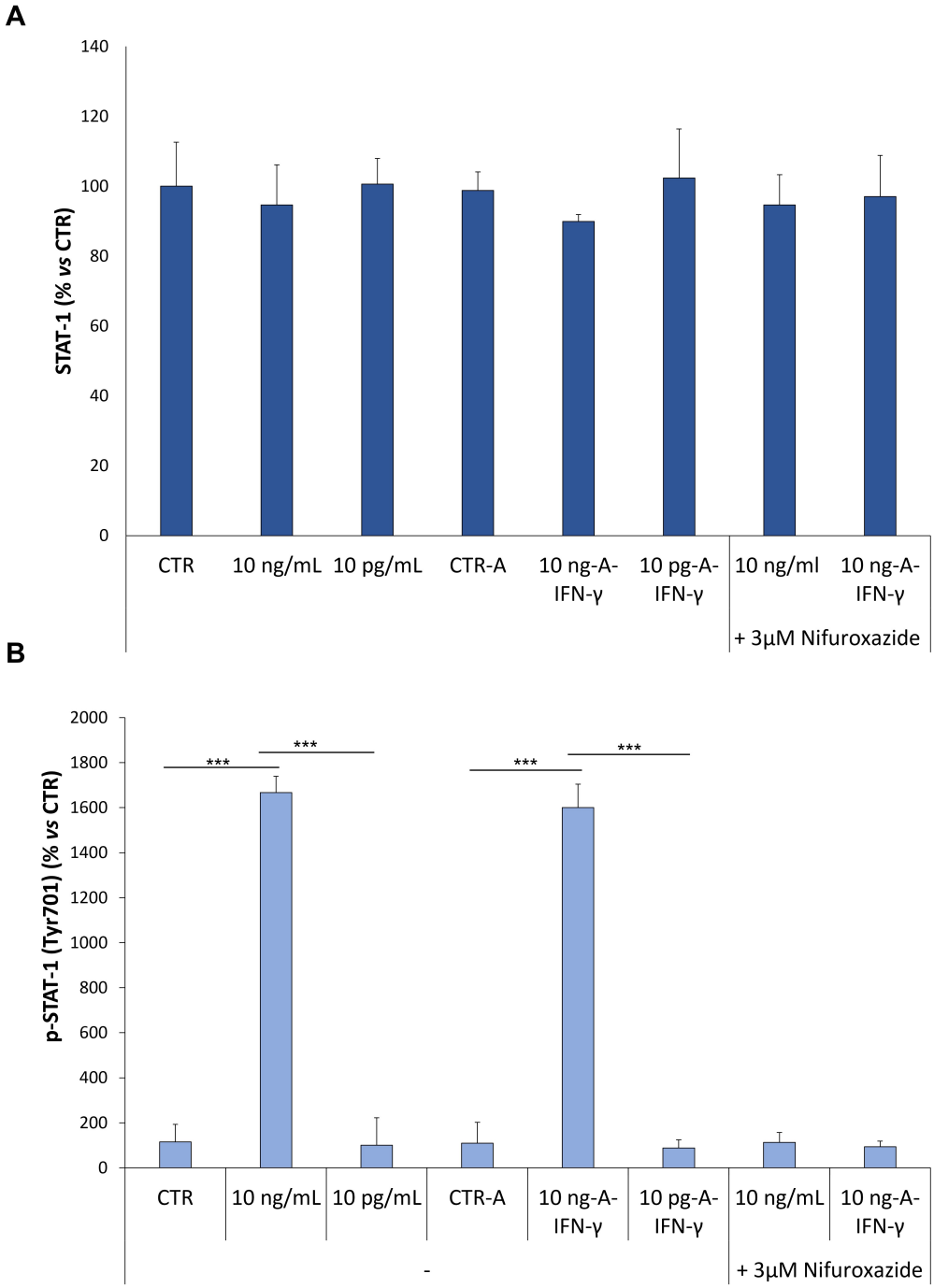

Fig. 1. Pharmacological concentrations of interferon (IFN)-γ activates the Signal transducer and activator of transcription (STAT) pathway. Human Umbilical Vein Endothelial Cells (HUVEC) were treated for 30 min with pharmacological (10 ng/mL) or low (10 pg/mL) concentrations of IFN-γ, subjected or not to activation. (A) The total amounts of STAT-1 were measured by enzyme linked immunosorbent assay (ELISA). (B) The phosphorylation of STAT-1 (p-STAT-1) was evaluated by ELISA. The experiment was performed three times in triplicate ± standard deviation (SD). The data were analysed using two-way one-way analysis of variance (one-way ANOVA). *** $p \leq 0.001$. CTR: physiological solution; CTR-A: activated physiological solution; 10 ng-A-IFN-γ: pharmacological concentration of activated IFN-γ; 10 pg-A-IFN-γ: low dose activated IFN-γ.

Journal of
BIOLOGICAL REGULATORS
and Homeostatic Agents

idase (dilution 1:4000, anti-rabbit Catalogue no. NA934, anti-mouse Catalogue no. NXA931, Amersham Pharmacia Biotech Italia, Cologno Monzese, Italy) were used. The immunoreactive proteins were detected with Clarity™ Western ECL substrate (Catalogue no. 1705060, Bio-Rad, Hercules, CA, USA) and images were captured with a Chemi-Doc MP Imaging System (Bio-Rad, Hercules, CA, USA). Densitometry of the bands was performed with the software ImageJ (version 1.54d, National Institute of Health, Bethesda, MD, USA). The Western blots shown are representative and the densitometric analysis was performed on three independent experiments ± standard deviation (SD).

ELISA

The PathScan® PHOSPHO-STAT-1 (Tyr701) (Catalogue no. 7234, Cell Signaling, Pero, MI, Italy) and PathScan® RP Total STAT-1 Sandwich enzyme linked immunosorbent assay (ELISA) Kits (Catalogue no. 25253, Cell Signaling, Pero, MI, Italy) were used to measure the activation of STAT-1 according to the manufacturer's instructions. InstantOne ELISA ERK1/2 (Total/Phospho) (Catalogue no. 85-86013-11, Thermo Fisher Scientific, Waltham, MA, USA) was used to analyse ERK1/2 phosphorylation according to the manufacturer's instructions. All ELISAs were performed three times, and each sample was measured in triplicate.

Migration Assay

Cell migration was determined using an *in vitro* model of wound repair as previously described [30]. 10×10^4 HUVEC were cultured in 24-well plates to confluence. After 16 h of starvation in medium without fetal bovine serum and endothelial cell growth factor (ECGF), the monolayer was wounded and treated with pharmacological or low-dose concentrations of IFN-γ for 24 h. Vascular endothelial growth factor (VEGF) (10 ng/mL, 100-20, PeproTech, London, UK) was used as positive control. The cells were stained with crystal violet to visualize the width of the wound, and images were captured with a 4× objective using a phase contrast microscope [26]. The wound area was calculated by ImageJ software and expressed using an arbitrary value scale. The cells were also fixed in phosphate buffered saline containing 4% paraformaldehyde and 2% sucrose (pH 7.6) and stained with rhodamine-labelled phalloidin (Catalogue no. R415, Thermo Fisher Scientific, Waltham, MA, USA) and 4′,6-diamidino-2-phenylindole (DAPI) (Catalogue no. D1306, Thermo Fisher Scientific, Waltham, MA, USA) to visualize the cytoskeleton and the nuclei, respectively. The images were acquired using 20× objective by EVOS Floid Cell Imaging Station (Catalog no. 4471136, Thermo Fisher Scientific, Waltham, MA, USA). In some experiments, after starvation for 15 h, HUVEC were exposed to 30 µM ERK inhibitor III (Calbiochem, San Diego, CA, USA) for 1 h before performing the wound and the treatment with IFN-γ for additional 24 h. To obtain a transient downregulation of ERK1/2 in HUVEC, we used Lipofectamine RNAiMAX (Catalogue no. 13778075, Thermo Fisher Scientific, Waltham, MA, USA) according to the manufacturer's recommendations in combination with the stealth siRNAs for *ERK1/2* (MAPK1/ERK2 Catalogue no. 1027416; MAPK3/ERK1 Catalogue no.1027416, Qiagen, Hilden, Germany). The sequences used are reported in Table 1. Non-silencing, scrambled sequences were used as controls. Transfection with siRNAs was performed in starvation medium for 16 h before wounding and treating with IFN-γ for 24 h. At the end of the experiment, the wound area was calculated by ImageJ software (version 1.54d, National Institute of Health, Bethesda, MD, USA) on crystal violet - stained cells and expressed using an arbitrary value scale. The experiments were performed three times in triplicate. Data are shown as the mean ± SD.

Table 1. The sequences of the siRNAs used are reported.

GENE	SEQUENCES 3′ ⟶ 5′
MAPK1/ERK2	AAGTTCGAGTAGCTATCAAGA
	AACACTTGTCAAGAAGCGTTA
	AATGACATTATTCGAGCACCA
	ATCATGGTAGTCACTAACATA
MAPK3/ERK1	CTCCCTGACCCGTCTAATATA
	CCCGTCTAATATATAAATATA
	CAAGACTCGCGTGGCCATCAA
	TGGACCGGATGTTAACCTTTA

MAPK, Mitogen-activated protein kinase; *ERK*, Extracellular signal-regulated kinase; siRNA, short interfering RNA.

Statistical Analysis

Data are expressed as the mean ± SD. In the experiments in which the cells were treated only with the different concentrations of IFN-γ, the data were analysed using one-way analysis of variance (one-way ANOVA). When the cells were treated with different concentrations of IFN-γ in the presence of other experimental conditions (3 µM Nifuroxazide; siRNA ERK; ERK III inhibitor), the data were analysed using two-way ANOVA. The *p*-values deriving from multiple pairwise comparisons were corrected using the Bonferroni method. Statistical significance was defined as p-value ≤ 0.05. In the figures, ** $p \leq 0.01$; *** $p \leq 0.001$. The graph containing the complete statistical analysis is available in the supplementary.

Results

Low-Dose A-IFN-γ Does Not Phosphorylate STAT-1

Initially, we evaluated STAT-1 in HUVEC exposed to pharmacological or low-dose concentrations of IFN-γ, both activated and non-activated, for 30 min. No modulation of the total amounts of STAT-1 was detected by ELISA (Fig. 1A). Fig. 1B shows that 30 min of treatment with

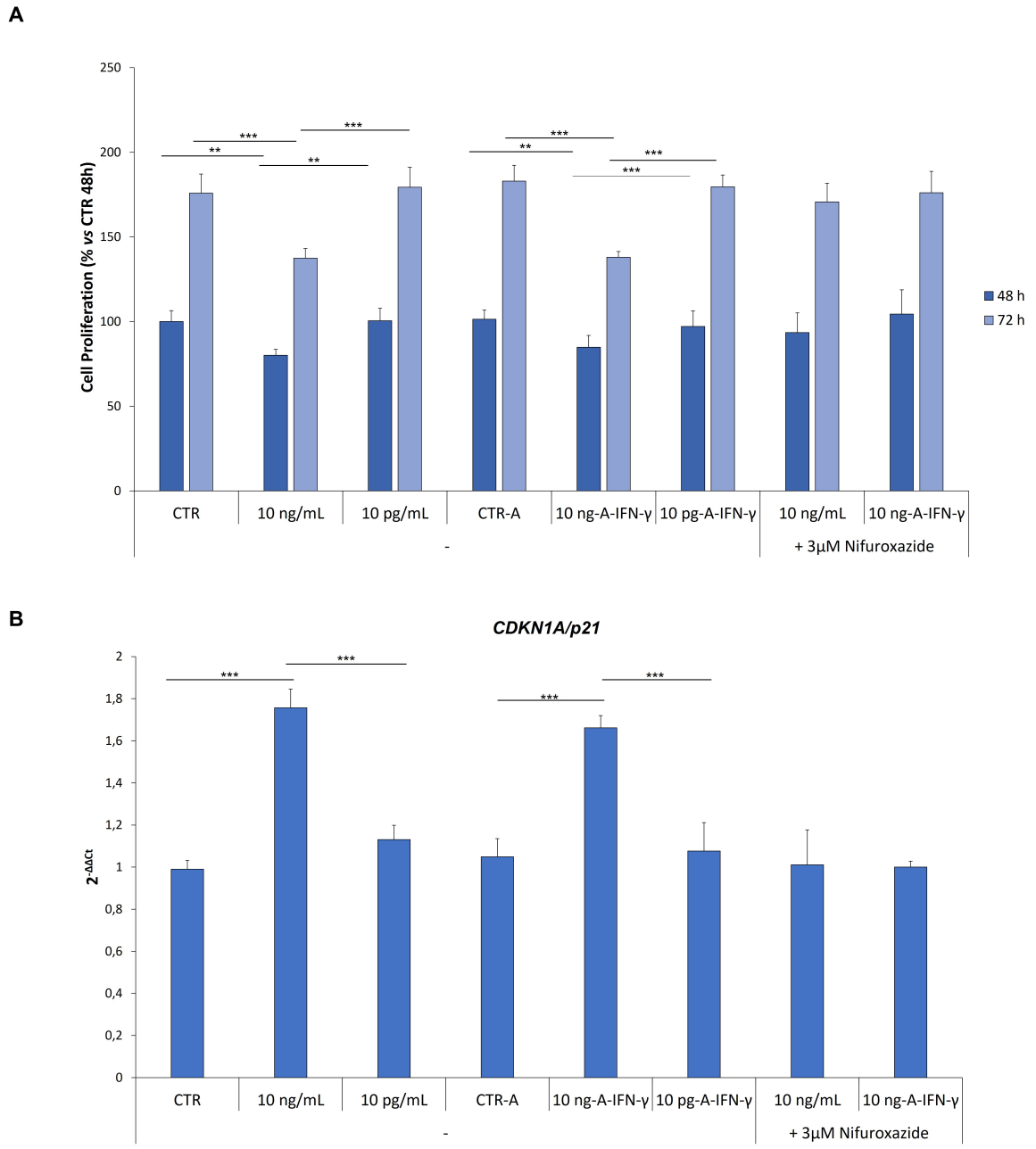

Fig. 2. Pharmacological concentrations of IFN-γ inhibit HUVEC proliferation. HUVEC were treated with pharmacological (10 ng/mL) or low (10 pg/mL) concentrations of IFN-γ, subjected or not to activation. (A) The cells were counted after 48 and 72 h. The results are the mean of four separate experiments performed in triplicate. (B) After 16 h of treatment, Real-time Quantitative Reverse Transcription PCR (qRT-PCR) was performed on RNA extracted from the cells as described in the methods. The experiments were performed three times in triplicate ± SD. The y axis refers to the method used in order to calculate the relative fold gene expression of sample ($2^{-\Delta\Delta Ct}$ method). The data were analysed using two-way ANOVA. ** $p \leq 0.01$; *** $p \leq 0.001$. CTR: physiological solution; CTR-A: activated physiological solution; 10 ng-A-IFN-γ: pharmacological concentration of activated IFN-γ; 10 pg-A-IFN-γ: low dose activated IFN-γ.

10 ng/mL non-activated or activated IFN-γ (10 ng/mL or 10 ng-A-IFN-γ) induced STAT-1 phosphorylation, an event that was prevented when the cells were pre-treated for 16 h with the STAT inhibitor nifuroxazide (3 μM). Conversely, no phosphorylation of STAT-1 was observed after treating HUVEC with non-activated or activated low-dose IFN-γ (10 pg/mL or 10 pg-A-IFN-γ) (Fig. 1B). Similar results were obtained with (activated physiological solution (CTR-A)) and non activated physiological solutions (CTR).

Journal of
BIOLOGICAL REGULATORS
and Homeostatic Agents

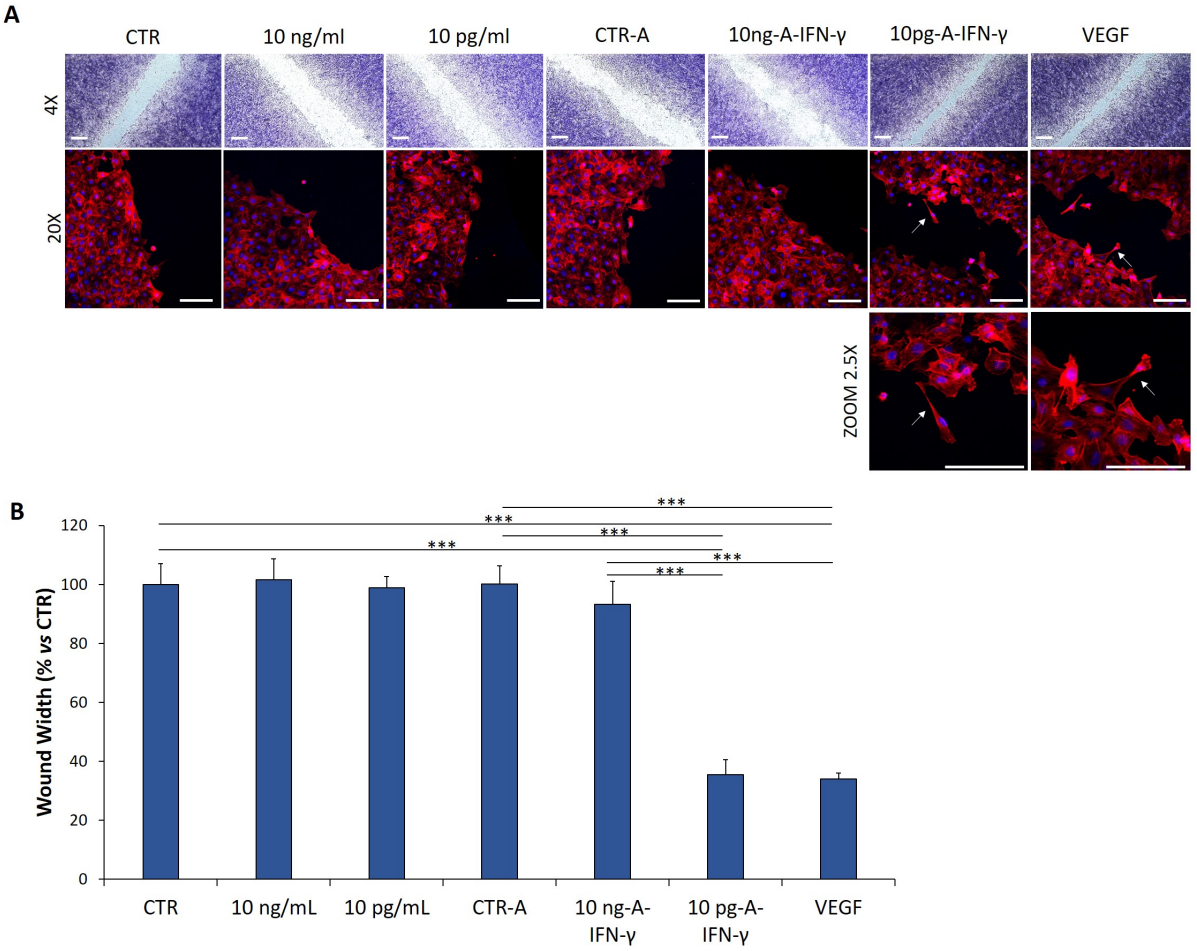

Fig. 3. Low-dose A-IFN-γ induces HUVEC migration. HUVEC were grown in 24-well plates to confluence. After 16 h of starvation, the monolayer was wounded and the cells were treated with pharmacological (10 ng/mL) or low (10 pg IFN-γ) concentrations of IFN-γ, subjected or not to activation. Vascular endothelial growth factor (VEGF) (10 ng/mL) was used as a positive control. (A) After 24 h, the cells were stained with crystal violet and images acquired with a 4× objective using a phase contrast microscope (upper panel). Scale bar: 250 µm. Cytoskeleton was visualized after staining with fluorescein-labeled phalloidin and nuclei with 4′,6-diamidino-2-phenylindole (DAPI). The images were acquired using the 20× objective of Floid imaging Station (lower panel). Scale bar: 100 µm. A representative experiment is shown. The white arrows indicate the cells with a migratory phenotype, which are magnified (zoom 2.5×) in the lower box. Scale bar: 100 µm. (B) The wound area was calculated by ImageJ software using images with cells stained with crystal violet. Data are shown as the mean of three experiments ± SD. The data were analysed using one-way ANOVA. *** $p \leq 0.001$. CTR: physiological solution; CTR-A: activated physiological solution; 10 ng-A-IFN-γ: pharmacological concentration of activated IFN-γ; 10 pg-A-IFN-γ: low dose activated IFN-γ.

Low-Dose A-IFN-γ Does Not Affect HUVEC Proliferation

We compared the proliferative response of HUVEC exposed either to pharmacological (10 ng/mL) or low (10 pg/mL) concentrations of IFN-γ, activated or not. While 10 pg/mL IFN-γ or A-IFN-γ exerted no effects (Fig. 2A), 10 ng/mL IFN-γ, both activated or not, inhibited HUVEC proliferation and induced the expression of the cyclin-dependent kinase inhibitor 1A/p21 (*CDKN1A*/*p21*), which codes for p21, as detected by qRT-PCR (Fig. 2B). Nifuroxazide (3 µM) prevented growth inhibition and *CDKN1A*/p21 expression in HUVEC treated with 10 ng/mL IFN-γ, subjected or not to activation (Fig. 2A,B).

Low-Dose A-IFN-γ Increases HUVEC Migration

We then analysed endothelial migration in HUVEC cultured in the presence of pharmacological or low-dose concentrations of IFN-γ for 24 h. VEGF (10 ng/mL) was used as positive control [31]. Fig. 3A shows a representa-

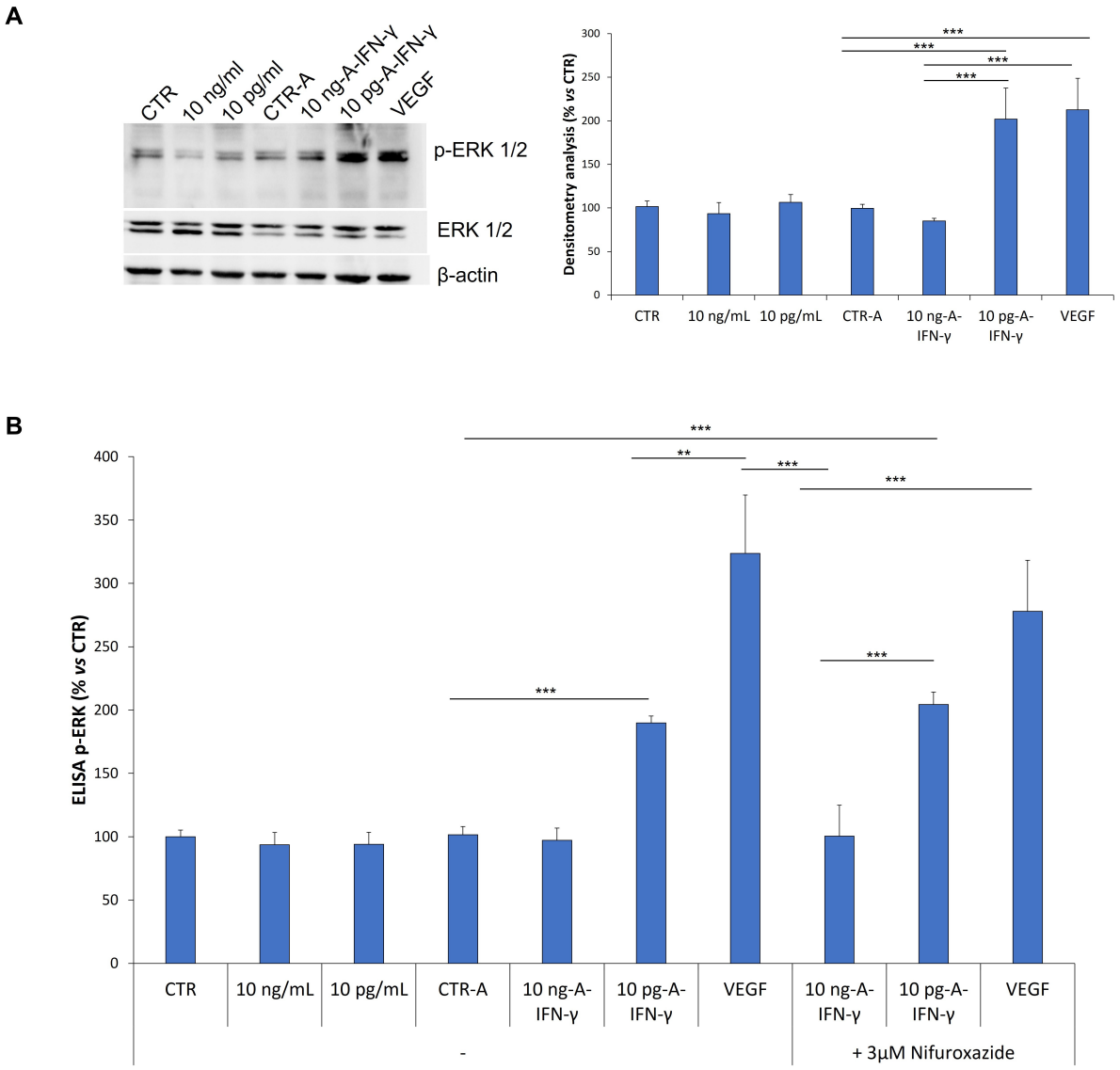

Fig. 4. Low-dose A-IFN-γ activates Extracellular signal-regulated kinase (ERK) signalling. After 16 h of starvation, HUVEC were treated for 30 min with the different concentrations of IFN-γ. Then the cells were lysed and the phosphorylation of ERK1/2 was analyzed by western blot (A) and ELISA (B). Actin was used as a control of loading. A representative blot and densitometry obtained by ImageJ on three independent experiments ± SD are shown. The data were analysed using one-way ANOVA. The ELISA results are the mean of three experiments in triplicates ± SD. The data were analysed using two-way ANOVA. ** $p \leq 0.01$; *** $p \leq 0.001$. CTR: physiological solution; CTR-A: activated physiological solution; 10 ng-A-IFN-γ: pharmacological concentration of activated IFN-γ; 10 pg-A-IFN-γ: low dose activated IFN-γ.

tive experiment after staining the cells with crystal violet. The cells were also stained with rhodamine-labelled phalloidin to detect the cytoskeleton and DAPI to visualize the nuclei. 10 pg-A-IFN-γ and VEGF induced polarized cell elongation (highlighted by the white arrows and magnified in the lower box), which is typical of the endothelial migratory phenotype [30,32]. Quantification of the wound width is reported in Fig. 3B, which shows that 10 pg-A-IFN-γ increased HUVEC migration. Interestingly, HUVEC migration was not modulated by non activated low-dose IFN-γ or pharmacological concentrations of IFN-γ.

Journal of
BIOLOGICAL REGULATORS
and Homeostatic Agents

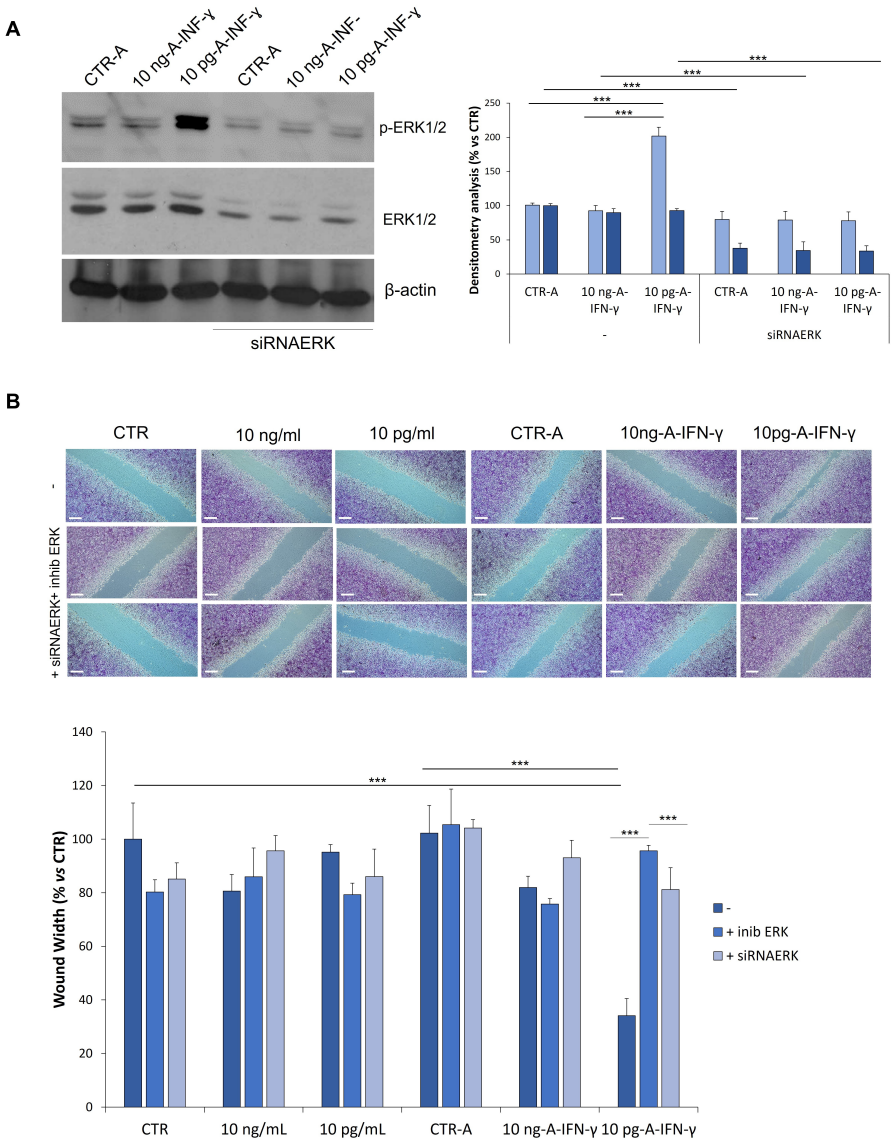

Fig. 5. ERK inhibition blocks HUVEC migration induced by low-dose A-IFN-γ. HUVEC were grown in 24-well plates to confluence and wound assay was performed in HUVEC treated with the ERK inhibitor III (30 μM) or silenced for *ERK* as described in the methods. (A) The silencing of *ERK1/2* was evaluated by western blot (left panel). Actin was used as a control of loading. A representative blot and densitometry obtained by ImageJ on three independent experiments ± SD are shown. (B) Cells were stained with crystal violet and the images were acquired with a 4× objective using a phase contrast microscope (upper panel). Scale bar: 250 μm. The wound area was calculated by ImageJ software (lower panel). The experiments were performed in triplicate. Data are shown as the mean ± SD. The data were analysed using two-way ANOVA. *** $p \leq 0.001$. CTR: physiological solution; CTR-A: activated physiological solution; 10 ng-A-IFN-γ: pharmacological concentration of activated IFN-γ; 10 pg-A-IFN-γ: low dose activated IFN-γ.

Low-Dose A-IFN-γ Activates ERK

We analysed whether ERK was activated in HUVEC treated with 10 pg/mL IFN-γ or A-IFN-γ. Both western blot and ELISA demonstrate that only 10 pg/mL of A-IFN-γ induced ERK phosphorylation (Fig. 4 A,B). VEGF (10 ng/mL) was used as a positive control. ERK was not

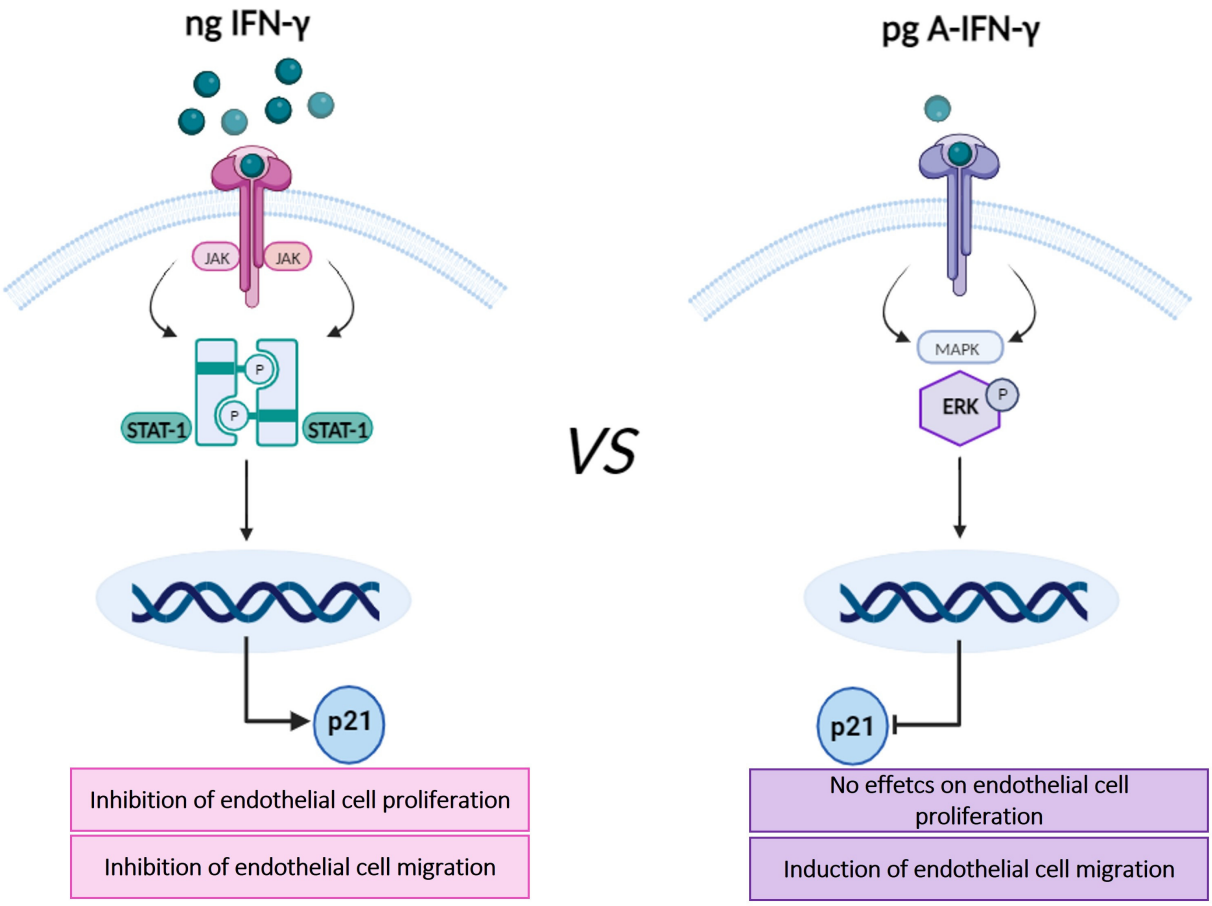

Fig. 6. The mechanisms of action of pharmacological *vs* low-dose A- IFN-γ. The cartoon is created by Biorender.com to summarize the findings of our work.

phosphorylated neither by pharmacological concentration of IFN-γ nor by 10 pg/mL non activated IFN-γ. As expected, Nifuroxazide had no effects on ERK phosphorylation of the samples (Fig. 4B).

ERK Mediates the Increase of Endothelial Migration after Treatment with Low-Dose A-IFN-γ

To understand the role of ERK in mediating low-dose A-IFN-γ-induced HUVEC migration, we inhibited ERK by using a specific pharmacological inhibitor, i.e., ERK inhibitor III, and by silencing ERK using specific siRNA. The efficiency of siRNA ERK was evaluated by western blot, demonstrating the marked downregulation of the proteins (Fig. 5A). We then analysed cell migration in the presence of pharmacological or low-dose concentrations of IFN-γ in HUVEC treated with ERK inhibitor III or silenced with siRNA. ERK inhibition prevented the increase of HUVEC migration induced by low-dose A-IFN-γ (Fig. 5B).

Discussion

The use of low-dose activated cytokines is taking its first steps in *in vitro* studies as well as in clinical settings [33,34]. In *vivo*, the principal aim is the harmonization of cellular function to maintain or restore homeostasis. Different activated cytokines have yielded promising results in patients with psoriasis [35], atopic dermatitis [36] and rheumatoid arthritis [37]. Concerning IFN-γ, low-doses of A-IFN-γ potentiated the activity of natural killer cells isolated from patients with early-stage colon cancer [38]. In Jurkat cells, low-dose A-IFN-γ exerted an immunomodulatory action by tuning signal transduction and gene expression [26].

Here we compare the effects of pharmacological and low-dose IFN-γ, activated or not, in cultured EC. We show that pharmacological and low-dose A-IFN-γ exert different effects in HUVEC by activating distinct signal transduction pathways (Fig. 6). 10 ng/mL IFN-γ, subjected or not to activation, inhibited cell growth by upregulating the *CDKN1A/p21*, in agreement with previous results obtained in HUVEC [17] and other cell types [39]. It is known that

Journal of
BIOLOGICAL REGULATORS
and Homeostatic Agents

activated STAT-1 specifically binds the conserved STAT-responsive elements in the promoter of the gene encoding *CDKN1A/p21*, resulting in the overexpression of its RNA. In brief, it is STAT-1 activation that mediates IFN-γ-dependent growth inhibition, as demonstrated in HUVEC exposed to siRNA targeting *STAT-1* [17]. This result is in agreement with our data showing that the STAT inhibitor prevents the effects of 10 ng/mL IFN-γ in HUVEC. Additionally, the evidence that 10 pg/mL of IFN-γ, which did not activate STAT-1, had no impact on cell proliferation or the expression of *CDKN1A/p21*, further supports this finding. Intriguingly, only low-dose A-IFN-γ stimulates HUVEC migration, and this happens through the activation of ERK. Indeed, siRNA targeting ERK as well as the ERK inhibitor III prevent the stimulation of cell migration induced by low-dose A-IFN-γ. It is noteworthy that ERK is central in endothelial migration, as shown in primary endothelial cells derived from ERK knock out mice [40].

Two main questions arise at this point. The first question pertains to the involvement of ERK in the signal cascade, and the second one concerns the need for kinetic activation of the low-dose cytokine to potentiate its action. Although STAT-1 is essential in cell response to IFN-γ, several studies have also demonstrated the existence of STAT-1 independent pathways, often in a cell type specific fashion [41]. As examples, we recall that ERK is rapidly activated in IFN-γ treated neurons [41] and ERK-dependent STAT-1 phosphorylation maximizes STAT-1 activity in macrophages [42]. In EC long treatments with IFN-γ activate p38 Mitogen-activated protein kinase (MAPK), with consequent effects on cytoskeletal reorganization [18,43]. Therefore, it is known that ERK contributes to the signalling activated by pharmacological concentrations of IFN-γ. The novelty of our results lies in the evidence that low-dose A-IFN-γ rapidly activates ERK, mediating the stimulation of endothelial migration, rather than relying on the canonical STAT-1 pathway. We hypothesize that low-doses of A-IFN-γ unveil the involvement of the ERK pathway, which is otherwise overshadowed by the dominance of STAT-1 signalling.

Since pharmacological concentrations of IFN-γ not only inhibit growth but also stimulate apoptosis of HUVEC [44], while low concentrations guarantee normal proliferation rate and increase migration, we propose that these apparently conflicting results might be framed in the perspective of the hormetic dose responses, which means that low concentrations of potentially harmful molecules exert beneficial effects [45]. Hormesis is now envisioned as an adaptive cellular response which contributes to the maintenance of homeostasis by enhancing biologic plasticity [46]. Since the exceptional sensitivity to low concentrations of ligands is maintained from unicellular to mammalian organisms, hormesis might have played an important role in evolution as a survival strategy [23].

It should be noted that most of the experimental studies are conducted using concentrations much higher than those detected *in vivo* [20–22]. Regarding IFN-γ, the average serum concentration in healthy adults ranges from 2 to 10 pg/mL [47,48]. In experimental studies, nanograms of IFN-γ are generally utilized. The quantitative insight into the number of molecules needed to activate a target cell has not attracted much attention until recently, and evidence is beginning to accumulate about the effects of low-doses of biological active compounds [23]. An example comes from studies on relaxin, which has been shown to be active in a wide range of doses, spanning from attomolar to millimolar concentrations [49]. This phenomenon might be attributed to the relaxin receptor, a G-protein coupled receptor, which preassembles into a large signalling complex, thereby facilitating its activation by very low concentrations of relaxin [49]. On these bases, we speculate that low-dose A-IFN-γ might stimulate ERK phosphorylation by binding to particular domains of the plasma membrane enriched in IFN-γ receptors. Also cytokines trigger cellular responses [23,48] at femto to picomolar concentrations. IL-6 signalling requires only a few IL-6 molecules to exert its biological activity in B9 hybridoma cells [24]. A recent study suggests that picograms of IFN-γ stimulate the proliferation, the activation and the secretion of cytokines by immune cells [48].

It remains unclear and challenging to explain why only low-dose A-IFN-γ activates ERK and stimulates HUVEC migration. These results are consistent with the findings of Gariboldi *et al.* [28], who were the first to observe differences in the activity of activated *vs* not-activated low dose cytokine solutions in a murine model of asthma. It has been shown that mechanical exposure alters the physical-chemical characteristics of water with consequences on the infrared emission spectra of ultra-high diluted IFN-γ solutions [50]. Based on these findings, we hypothesize that mechanical forces might induce conformational changes of IFN-γ itself, optimizing its binding to its receptor and maximizing cell response. Further studies are warranted to elucidate the mechanisms involved in this intriguing, yet mysterious model of immunological stimulation, which is yielding promising results also in clinical settings [33,35,36,51].

Conclusions

In conclusion, in HUVEC, STAT-1 serves as the principal intracellular signal activated by nanograms of IFN-γ, independently of mechanical stimulation, whereas the activation of ERK mediates the increase of endothelial migration in response to low-dose A-IFN-γ (Fig. 6).

Availability of Data and Materials

The data presented in this study are openly available in Dataverse through the following link: https://dataverse.unimi.it/dataverse/IFNg.

Author Contributions

VM, SC and JAM designed the research study. AC performed the research. AC, SC analyzed the data. JAM wrote the manuscript. All authors contributed to editorial changes in the manuscript. All authors read and approved the final manuscript. All authors have participated sufficiently in the work and agreed to be accountable for all aspects of the work.

Ethics Approval and Consent to Participate

Not applicable.

Acknowledgment

Not applicable.

Funding

This study received funding from Guna S.p.a. The funder was not involved in the study design, collection, analysis, interpretation of data, the writing of this article or the decision to submit it for publication.

Conflict of Interest

Vincenzo Miranda is employed by Guna S.p.a., Italy. Jeanette A. Maier is serving as one of the Editorial Board of this journal. We declare that Vincenzo Miranda and Jeanette A. Maier had no involvement in the peer review of this article and has no access to information regarding its peer review. The other authors declare no conflict of interest.

References

[1] Turner NA, Moake J. Assembly and activation of alternative complement components on endothelial cell-anchored ultra-large von Willebrand factor links complement and hemostasis-thrombosis. PloS One. 2013; 8: e59372.

[2] Mai J, Virtue A, Shen J, Wang H, Yang XF. An evolving new paradigm: endothelial cells–conditional innate immune cells. Journal of Hematology & Oncology. 2013; 6: 61.

[3] Castro F, Cardoso AP, Gonçalves RM, Serre K, Oliveira MJ. Interferon-Gamma at the Crossroads of Tumor Immune Surveillance or Evasion. Frontiers in Immunology. 2018; 9: 847.

[4] Bhat MY, Solanki HS, Advani J, Khan AA, Keshava Prasad TS, Gowda H, *et al*. Comprehensive network map of interferon gamma signaling. Journal of Cell Communication and Signaling. 2018; 12: 745–751.

[5] Majoros A, Platanitis E, Kernbauer-Hölzl E, Rosebrock F, Müller M, Decker T. Canonical and Non-Canonical Aspects of JAK-STAT Signaling: Lessons from Interferons for Cytokine Responses. Frontiers in Immunology. 2017; 8: 29.

[6] Bluyssen HA, Muzaffar R, Vlieststra RJ, van der Made AC, Leung S, Stark GR, *et al*. Combinatorial association and abundance of components of interferon-stimulated gene factor 3 dictate the selectivity of interferon responses. Proceedings of the National Academy of Sciences of the United States of America. 1995; 92: 5645–5649.

[7] Gil MP, Bohn E, O'Guin AK, Ramana CV, Levine B, Stark GR, *et al*. Biologic consequences of Stat1-independent IFN signaling. Proceedings of the National Academy of Sciences of the United States of America. 2001; 98: 6680–6685.

[8] Green DS, Young HA, Valencia JC. Current prospects of type II interferon γ signaling and autoimmunity. The Journal of Biological Chemistry. 2017; 292: 13925–13933.

[9] Indraccolo S, Pfeffer U, Minuzzo S, Esposito G, Roni V, Mandruzzato S, *et al*. Identification of genes selectively regulated by IFNs in endothelial cells. Journal of Immunology (Baltimore, Md.: 1950). 2007; 178: 1122–1135.

[10] Chen W, Shen L, Jiang J, Zhang L, Zhang Z, Pan J, *et al*. Antiangiogenic therapy reverses the immunosuppressive breast cancer microenvironment. Biomarker Research. 2021; 9: 59.

[11] Jorgovanovic D, Song M, Wang L, Zhang Y. Roles of IFN-γ in tumor progression and regression: a review. Biomarker Research. 2020; 8: 49.

[12] Sun T, Yang Y, Luo X, Cheng Y, Zhang M, Wang K, *et al*. Inhibition of tumor angiogenesis by interferon-γ by suppression of tumor-associated macrophage differentiation. Oncology Research. 2014; 21: 227–235.

[13] Kammertoens T, Friese C, Arina A, Idel C, Briesemeister D, Rothe M, *et al*. Tumour ischaemia by interferon-γ resembles physiological blood vessel regression. Nature. 2017; 545: 98–102.

[14] Franco CA, Jones ML, Bernabeu MO, Geudens I, Mathivet T, Rosa A, *et al*. Dynamic endothelial cell rearrangements drive developmental vessel regression. PLoS Biology. 2015; 13: e1002125.

[15] Bodnar RJ, Yates CC, Rodgers ME, Du X, Wells A. IP-10 induces dissociation of newly formed blood vessels. Journal of Cell Science. 2009; 122: 2064–2077.

[16] Ashkar AA, Di Santo JP, Croy BA. Interferon gamma contributes to initiation of uterine vascular modification, decidual integrity, and uterine natural killer cell maturation during normal murine pregnancy. The Journal of Experimental Medicine. 2000; 192: 259–270.

[17] Battle TE, Lynch RA, Frank DA. Signal transducer and activator of transcription 1 activation in endothelial cells is a negative regulator of angiogenesis. Cancer Research. 2006; 66: 3649–3657.

[18] Sonar SA, Shaikh S, Joshi N, Atre AN, Lal G. IFN-γ promotes transendothelial migration of $CD4^+$ T cells across the blood-brain barrier. Immunology and Cell Biology. 2017; 95: 843–853.

[19] Ng CT, Fong LY, Sulaiman MR, Moklas MAM, Yong YK, Hakim MN, *et al*. Interferon-Gamma Increases Endothelial Permeability by Causing Activation of p38 MAP Kinase and Actin Cytoskeleton Alteration. Journal of Interferon & Cytokine Research: the Official Journal of the International Society for Interferon and Cytokine Research. 2015; 35: 513–522.

[20] Lu MY, Huang CI, Dai CY, Wang SC, Hsieh MY, Hsieh MH, *et al*. Elevated on-treatment levels of serum IFN-gamma is associated with treatment failure of peginterferon plus ribavirin therapy for chronic hepatitis C. Scientific Reports. 2016; 6: 22995.

[21] Lauw FN, Simpson AJ, Prins JM, Smith MD, Kurimoto M, van Deventer SJ, *et al*. Elevated plasma concentrations of interferon (IFN)-gamma and the IFN-gamma-inducing cytokines interleukin (IL)-18, IL-12, and IL-15 in severe melioidosis. The Journal of Infectious Diseases. 1999; 180: 1878–1885.

[22] Oke V, Gunnarsson I, Dorschner J, Eketjäll S, Zickert A, Niewold TB, *et al*. High levels of circulating interferons type I, type II and type III associate with distinct clinical features of active systemic lupus erythematosus. Arthritis Research & Therapy. 2019; 21: 107.

[23] Calabrese EJ, Giordano J. Ultra low doses and biological amplification: Approaching Avogadro's number. Pharmacological Research. 2021; 170: 105738.

[24] Hansen MB. Interleukin-6 signaling requires only few IL-6 molecules: Relation to physiological concentrations of extracellular IL-6. Immunity, Inflammation and Disease. 2020; 8: 170–180.

[25] Kak G, Raza M, Tiwari BK. Interferon-gamma (IFN-γ): Exploring its implications in infectious diseases. Biomolecular Concepts. 2018; 9: 64–79.

[26] Castiglioni S, Miranda V, Cazzaniga A, Campanella M, Nichelatti M, Andena M, *et al*. Femtograms of Interferon-γ Suffice to Modulate the Behavior of Jurkat Cells: A New Light in Immunomodulation. International Journal of Molecular Sciences. 2017; 18: 2715.

[27] Zec S, Boskovic S. Cerium silicates formation from mechanically activated oxide mixtures. Journal of Materials Science. 2004; 39: 5283–5286.

[28] Gariboldi S, Palazzo M, Zanobbio L, Dusio GF, Mauro V, Solimene U, *et al*. Low dose oral administration of cytokines for treatment of allergic asthma. Pulmonary Pharmacology & Therapeutics. 2009; 22: 497–510.

[29] Zhao J, Nakahira K, Kimura A, Kyotani Y, Yoshizumi M. Up-regulation of iNOS Protects Cyclic Mechanical Stretch-Induced Cell Death in Rat Aorta Smooth Muscle Cells. International Journal of Molecular Sciences. 2020; 21: 8660.

[30] Baldoli E, Maier JAM. Silencing TRPM7 mimics the effects of magnesium deficiency in human microvascular endothelial cells. Angiogenesis. 2012; 15: 47–57.

[31] Weddell JC, Chen S, Imoukhuede PI. VEGFR1 promotes cell migration and proliferation through PLCγ and PI3K pathways. NPJ Systems Biology and Applications. 2017; 4: 1.

[32] Norton KA, Popel AS. Effects of endothelial cell proliferation and migration rates in a computational model of sprouting angiogenesis. Scientific Reports. 2016; 6: 36992.

[33] Bernasconi S. Low Dose Medicine: theoretical background and scientific evidence. Italian Journal of Pediatrics. 2018; 44: 23.

[34] Jacques C, Floris I, Lejeune B. Ultra-Low Dose Cytokines in Rheumatoid Arthritis, Three Birds with One Stone as the Rationale of the 2LARTH®Micro-Immunotherapy Treatment. International Journal of Molecular Sciences. 2021; 22: 6717.

[35] Roberti ML, Ricottini L, Capponi A, Sclauzero E, Vicenti P, Fiorentini E, *et al*. Immunomodulating treatment with low dose interleukin-4, interleukin-10 and interleukin-11 in psoriasis vulgaris. Journal of Biological Regulators and Homeostatic Agents. 2014; 28: 133–139.

[36] Carello R, Ricottini L, Miranda V, Panei P, Rocchi L, Arcieri R, *et al*. Long-term treatment with low-dose medicine in chronic childhood eczema: a double-blind two-stage randomized control trial. Italian Journal of Pediatrics. 2017; 43: 78.

[37] Martin-Martin LS, Giovannangeli F, Bizzi E, Massafra U, Ballanti E, Cassol M, *et al*. An open randomized active-controlled clinical trial with low-dose SKA cytokines versus DMARDs evaluating low disease activity maintenance in patients with rheumatoid arthritis. Drug Design, Development and Therapy. 2017; 11: 985–994.

[38] Radice E, Miranda V, Bellone G. Low-doses of sequential-kinetic-activated interferon-γ enhance the ex vivo cytotoxicity of peripheral blood natural killer cells from patients with early-stage colorectal cancer. A preliminary study. International Immunopharmacology. 2014; 19: 66–73.

[39] Chin YE, Kitagawa M, Su WC, You ZH, Iwamoto Y, Fu XY. Cell growth arrest and induction of cyclin-dependent kinase inhibitor p21 WAF1/CIP1 mediated by STAT1. Science (New York, N.Y.). 1996; 272: 719–722.

[40] Srinivasan R, Zabuawala T, Huang H, Zhang J, Gulati P, Fernandez S, *et al*. Erk1 and Erk2 regulate endothelial cell proliferation and migration during mouse embryonic angiogenesis. PloS One. 2009; 4: e8283.

[41] O'Donnell LA, Henkins KM, Kulkarni A, Matullo CM, Balachandran S, Pattisapu AK, *et al*. Interferon gamma induces protective non-canonical signaling pathways in primary neurons. Journal of Neurochemistry. 2015; 135: 309–322.

[42] Li N, McLaren JE, Michael DR, Clement M, Fielding CA, Ramji DP. ERK is integral to the IFN-γ-mediated activation of STAT1, the expression of key genes implicated in atherosclerosis, and the uptake of modified lipoproteins by human macrophages. Journal of Immunology (Baltimore, Md.: 1950). 2010; 185: 3041–3048.

[43] Ng CT, Fong LY, Abdullah MNH. Interferon-gamma (IFN-γ): Reviewing its mechanisms and signaling pathways on the regulation of endothelial barrier function. Cytokine. 2023; 166: 156208.

[44] Javanmard SH, Dana N. The effect of interferon γ on endothelial cell nitric oxide production and apoptosis. Advanced Biomedical Research. 2012; 1: 69.

[45] Mattson MP. Hormesis defined. Ageing Research Reviews. 2008; 7: 1–7.

[46] López-Otín C, Kroemer G. Hallmarks of Health. Cell. 2021; 184: 33–63.

[47] Kurtovic NO, Halilovic EK. Serum Concentrations of Interferon Gamma (IFN-γ) in Patients with Psoriasis: Correlation with Clinical Type and Severity of the Disease. Medical Archives (Sarajevo, Bosnia and Herzegovina). 2018; 72: 410–413.

[48] Jacques C, Chatelais M, Fekir K, Brulefert A, Floris I. The Unitary Micro-Immunotherapy Medicine Interferon-γ (4 CH) Displays Similar Immunostimulatory and Immunomodulatory Effects than Those of Biologically Active Human Interferon-γ on Various Cell Types. International Journal of Molecular Sciences. 2022; 23: 2314.

[49] Civciristov S, Ellisdon AM, Suderman R, Pon CK, Evans BA, Kleifeld O, *et al*. Preassembled GPCR signaling complexes mediate distinct cellular responses to ultralow ligand concentrations. Science Signaling. 2018; 11: eaan1188.

[50] Penkov N, Penkova N. Analysis of Emission Infrared Spectra of Protein Solutions in Low Concentrations. Frontiers in Physics. 2020; 8: 624779.

[51] Gough DJ, Levy DE, Johnstone RW, Clarke CJ. IFNgamma signaling-does it mean JAK-STAT? Cytokine & Growth Factor Reviews. 2008; 19: 383–394.